Biomacromolecules

pubs.acs.org/Biomac

Article

Effect of Radical Polymerization Method on Pharmaceutical Properties of Π Electron-Stabilized HPMA-Based Polymeric Micelles

Armin Azadkhah Shalmani,[#] Zaheer Ahmed,[#] Maryam Sheybanifard, Alec Wang, Marek Weiler, Eva Miriam Buhl, Geir Klinkenberg, Ruth Schmid, Wim Hennink, Fabian Kiessling, Josbert M. Metselaar, Twan Lammers,* Quim Peña,* and Yang Shi*

Cite This: *Biomacromolecules* 2023, 24, 4444−4453

Read Online

ACCESS | Metrics & More | Article Recommendations | Supporting Information

ABSTRACT: Polymeric micelles are among the most extensively used drug delivery systems. Key properties of micelles, such as size, size distribution, drug loading, and drug release kinetics, are crucial for proper therapeutic performance. Whether polymers from more controlled polymerization methods produce micelles with more favorable properties remains elusive. To address this question, we synthesized methoxy poly(ethylene glycol)-*b*-(*N*-(2-benzoyloxypropyl)-methacrylamide) (mPEG-*b*-p(HPMAm-Bz)) block copolymers of three different comparable molecular weights (∼9, 13, and 20 kDa), via both conventional free radical (FR) and reversible addition−fragmentation chain transfer (RAFT) polymerization. The polymers were subsequently employed to prepare empty and paclitaxel-loaded micelles. While FR polymers had relatively high dispersities ($Đ$ ∼ 1.5−1.7) compared to their RAFT counterparts ($Đ$ ∼ 1.1−1.3), they formed micelles with similar pharmaceutical properties (e.g., size, size distribution, critical micelle concentration, cytotoxicity, and drug loading and retention). Our findings suggest that pharmaceutical properties of mPEG-*b*-p(HPMAm-Bz) micelles do not depend on the synthesis route of their constituent polymers.

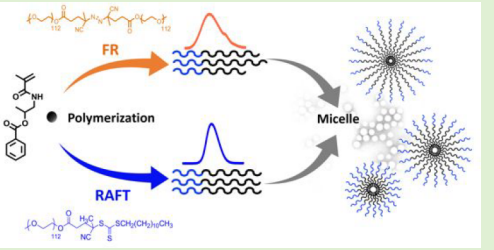

INTRODUCTION

Nanomedicines have demonstrated promise in enhancing the stability, bioavailability, target site accumulation and tolerability of active pharmaceutical ingredients.[1−3] Currently, there are around 60 clinically approved nanomedicines based on different types of nanocarriers such as liposomes, lipid nanoparticles, protein nanoparticles, and polymeric micelles.[4] Polymeric micelles are nanosized self-assemblies of amphiphilic block copolymers, composed of a hydrophilic shell and a hydrophobic core.[5] These nanocarriers are ideal drug delivery systems for poorly water-soluble cargoes,[6,7] including chemotherapeutic drugs such as taxanes, which are difficult to formulate.[8,9] Compared to other nanocarriers such as liposomes and lipid nanoparticles, polymeric micelles have better drug loading and retention capacities for hydrophobic drugs while having relatively small sizes, typically below 100 nm.[10]

Amphiphilic block copolymers used in micellar formulations can be synthesized using various polymerization approaches. For example, radical-based chain-growth polymerization strategies are ubiquitously employed for producing copolymers. In this context, conventional free radical (FR) and reversible addition−fragmentation chain transfer (RAFT) polymerizations are two of the most commonly applied techniques. FR polymerization is widely used in industrial setups and is known for its less controllable process and more polydisperse polymer products.[11] First introduced in 1998, RAFT employs chain transfer agents (CTA) to control the polymerization by oscillating the growing chains between active and dormant states, thereby producing polymers with better control of the molecular weight (MW) and narrower molecular weight distribution.[12,13] Such polymers may potentially meet higher quality standards from a pharmaceutical formulation point of view.

While numerous studies have employed different polymerization approaches to synthesize amphiphilic block copolymers for micelle preparation, the impact of the polymerization route on the properties of their resulting micelles is yet to be elucidated. Key pharmaceutical properties of polymeric micelles (such as size, polydispersity, drug loading and drug retention) are crucial for ensuring proper therapeutic performance.[14] It is intuitively assumed that polymers with a narrow molecular weight distribution, indicated by low dispersity ($Đ$), form micelles with narrower size distribution compared to polymers of broader molecular weight distribution. In a recent study by Buckinx et al., this assumption was challenged as they observed an inverse relationship between the dispersity of the

Special Issue: Polymers for Unmet Medical Challenges: Papers Presented at the Advanced Functional Polymers Medicine 2022 Conference

Received: October 22, 2022
Revised: January 19, 2023
Published: February 8, 2023

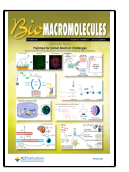

https://doi.org/10.1021/acs.biomac.2c01261
Biomacromolecules 2023, 24, 4444−4453

polymer and the size distribution of their nanoassemblies.[15] Here, we questioned whether self-assemblies of amphiphilic copolymers, synthesized by controlled radical polymerization compared to the conventional free radical method, are different from a pharmaceutical properties perspective.

In this study, we investigated whether the more controlled RAFT method produces polymers that form micelles with different size, size distribution, critical micelle concentration (CMC), cytotoxicity, and drug loading and retention properties as compared to FR polymerization. For this purpose, we employed RAFT and FR polymerization to synthesize methoxy poly(ethylene glycol)-*b*-(*N*-(2-benzoyloxypropyl)-methacrylamide) (mPEG-*b*-p(HPMAm-Bz)), which self-assembles into micelles with high colloidal stability and drug loading capacity via aromatic $\pi-\pi$ stacking interactions.[16,17] These polymers were used to prepare empty and paclitaxel (PTX)-loaded micelles to investigate, in a head-to-head comparison, the impact of conventional versus more controlled radical polymerization strategies on the pharmaceutical properties of the resulting micelles.

EXPERIMENTAL SECTION

Materials. 1-Aminopropan-2-ol, methacryloyl chloride, benzoyl chloride, *N*,*N*-dimethylpyridin-4-amine (DMAP), 4,4′-azobis(4-cyanopentanoic acid) (ABCPA), *N*,*N*′-dicyclohexylcarbodiimide (DCC), *N*,*N*-dimethylformamide (DMF), dimethyl sulfoxide (DMSO), dioxane, diethyl ether (Et_2O), tetrahydrofuran (THF), trifluoroacetic acid (TFA), dichloromethane (DCM), acetonitrile (ACN), 4-cyano-4-[(dodecylsulfanylthiocarbonyl)sulfanyl]pentanoic acid, poly(ethylene glycol) methyl ether (mPEG with M_n of 5000 Da), 2,2′-azobis(2-methylpropionitrile) (AIBN), and paclitaxel (PTX) were purchased from commercial suppliers in synthesis grade purity and used as received. The solvents used for the syntheses were synthesis grade and dried on 4 Å molecular sieves, except when directly purchased in anhydrous form.

Synthesis of *N*-(2-Benzoyloxypropyl) methacrylamide (HPMAm-Bz). HPMAm-Bz was synthesized as previously reported[18] by the coupling reaction of HPMAm and benzoyl chloride. HPMAm was also synthesized as reported previously,[18] by reacting 1-aminopropan-2-ol and methacryloyl chloride. Yield >70% (purity >95%). Elemental analysis calculated for $C_{14}H_{17}NO_3$: C, 68.03; H, 6.88; N, 5.58. Found: C, 68.05; H, 6.93; N, 5.66.

Synthesis of mPEG-ABCPA-mPEG. The macroinitiator was synthesized as previously reported by the esterification of ABCPA with mPEG,[18] and the product was further purified with acetone washes. Yield >80%.

Synthesis of Macro Chain Transfer Agent (macroCTA). The macroCTA (mPEG-CTA) was obtained based on adapted procedures from the literature,[19] via esterification of the RAFT CTA 4-cyano-4-[(dodecylsulfanylthiocarbonyl)sulfanyl]pentanoic acid and mPEG, using DCC as a coupling agent. mPEG (5.00 g, 1.00 mmol, 1 equiv) and CTA (0.484 g, 1.20 mmol, 1.20 equiv) were dissolved in DCM in a round-bottom flask and cooled using an ice−water bath. Furthermore, DCC (0.310 g, 1.50 mmol, 1.50 equiv) and DMAP (0.0134 mg, 0.12 mmol, 0.12 equiv) were dissolved in DCM and added dropwise to the solution containing mPEG and CTA with constant stirring under nitrogen atmosphere at 0 °C. The reaction mixture was stirred for 20 h at room temperature. The solution was filtered to remove the precipitated 1,3-dicyclohexyl urea (DCU), and the product was precipitated from the filtrate using Et_2O, collected by filtration, and dried under vacuum. Yield >70%.

Synthesis of mPEG-*b*-p(HPMAm-Bz) by FR Polymerization. mPEG-*b*-p(HPMAm-Bz) block copolymers were synthesized as reported previously,[17] using mPEG-ABCPA-mPEG as the macroinitiator and HPMAm-Bz as the monomer. Briefly, both the macroinitiator and monomer were dissolved in ACN with a monomer concentration of 300 mg/mL and three different molar ratios of macroinitiator:monomer (1:200, 1:100, and 1:50) to obtain block copolymers with different hydrophobic block lengths. The solutions were degassed by purging with nitrogen for 20 min followed by 18 h of reaction at 70 °C under nitrogen atmosphere. The resulting polymers were collected by precipitation in Et_2O and dried in vacuo. The products were analyzed by ^{1}H NMR and GPC.[20] The obtained block copolymers with a fixed PEG chain length (5 kDa) and three different hydrophobic block lengths are named large, medium, and small, respectively.

RAFT Polymerization of HPMAm-Bz. The RAFT polymerization conditions for HPMAm-Bz were assessed using 4-cyano-4-[(dodecylsulfanylthiocarbonyl)sulfanyl]pentanoic acid as CTA. The effect of solvent, monomer concentration, ratio of CTA:AIBN, as well as the ratio of CTA:monomer were evaluated by changing one parameter at a time and keeping others constant. HPMAm-Bz, CTA, and AIBN were dissolved in either DMSO or dioxane. The polymerization was performed in accordance with previous protocols.[21] The solutions were subjected to three consecutive rounds of freeze−pump−thaw for effective degassing. The reactions were performed at 70 °C in a preheated oil bath under nitrogen atmosphere. Aliquots were taken at different time points to monitor the monomer conversion (via ^{1}H NMR) and polymer MW (via GPC) over time.

Synthesis of mPEG-*b*-p(HPMAm-Bz) by RAFT Polymerization. For the synthesis of the block copolymers, HPMAm-Bz (989.2 mg, 4.00 mmol, 1 equiv), mPEG-CTA (216 mg, 0.04 mmol, 0.01 equiv), and AIBN (1.3 mg, 0.008 mmol, 0.002 equiv) were dissolved in 2 mL of DMSO. The solution was subjected to three consecutive rounds of freeze−pump−thaw for effective degassing, and the reaction was conducted at 70 °C in a preheated oil bath under nitrogen atmosphere. The polymerization was terminated at different time points to obtain polymers of different chain lengths, and the obtained polymers were collected and purified by precipitation in Et_2O three times. The polymers were dried under vacuum and analyzed by ^{1}H NMR and GPC.[20]

Kinetic Constant (*k*) Calculation for FR and RAFT Polymerizations. Kinetic constants (k) for each reaction under different conditions were calculated by considering the decrease of monomer concentration over time based on a first-order reaction kinetics and using eq 1, where M_0 is the starting monomer concentration, M_t is the monomer concentration at time t, and t is the time of reaction.

$$k = \frac{\ln\left(\frac{M_0}{M_t}\right)}{t} \quad (1)$$

Proton Nuclear Magnetic Resonance (^{1}H NMR) Spectroscopy. ^{1}H NMR data were recorded on Varian AV400 and AV600 instruments (Bruker Corporation). All NMR spectra were processed and analyzed using MestReNova 6.0. For monomer, macroCTA, and mPEG-*b*-p(HPMAm-Bz) block copolymers, DMSO-d_6 was used as the solvent. For the macroinitiator, $CDCl_3$ was employed.

Gel Permeation Chromatography (GPC). The number-average molecular weight (M_n), weight-average molecular weight (M_w), and dispersity ($Đ = M_w/M_n$) of the synthesized polymers were determined by GPC,[17] using a pre-column (PLgel 5 μm 50 × 7,5 mm, Agilent technologies) followed by two serial pLgel 5 μm MIXED-D columns (300 × 7.5 mm, Agilent technologies). PEGs of different MW and narrow molecular weight distribution (Agilent Technologies) were used as calibration standards. DMF containing 10 mM LiCl was used as eluent with a flow rate of 0.7 mL/min, and a temperature of 55 °C. The polymers were detected by a refractive index detector.

High-Performance Liquid Chromatography (HPLC). Analytical reversed-phase HPLC was performed using an Agilent HPLC system (1260 infinity II) equipped with a quaternary pump and UV−vis detector. For HPMA and HPMAm-Bz, a gradient elution method (Solvent A: H_2O/TFA (99.9/0.1% v/v); and Solvent B: ACN/TFA (99.9/0.1% v/v)) at a flow rate of 1 mL/min, injection volume of 1 μL and a C18 column (4.6 × 150 mm, particle size 5 μm) were used. The detection wavelength was 254 nm. **HPMAm**: (5−95% solvent B

https://doi.org/10.1021/acs.biomac.2c01261
Biomacromolecules 2023, 24, 4444−4453

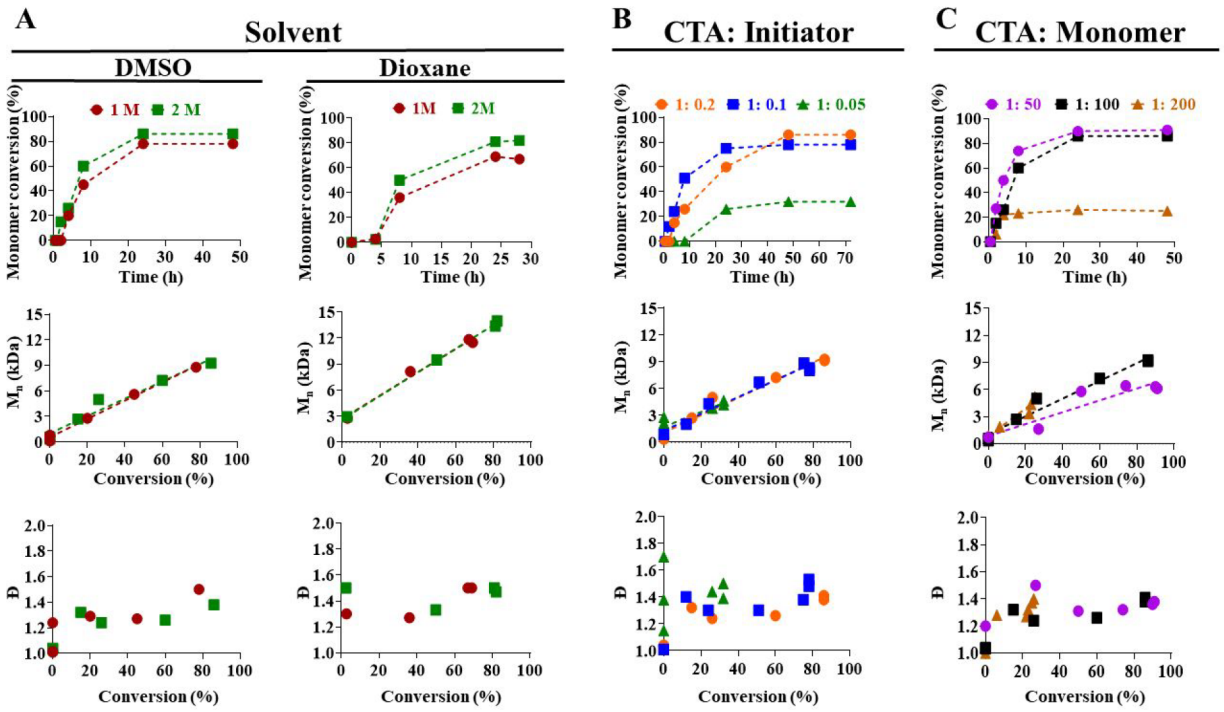

Figure 1. Effect of different reaction conditions on RAFT polymerization kinetics of HPMAm-Bz. Influence of different reaction conditions on monomer conversion (top) and the GPC-based M_n (middle) and dispersity ($Đ$) (bottom) of the resulting p(HPMAm-Bz) homopolymers. (A) Solvent (DMSO and dioxane) and monomer concentration (1 and 2 M). (B) Molar ratio of CTA to initiator (1:0.2, 1:0.1, and 1:0.05). (C) Molar ratio of CTA to monomer (1:50, 1:100, 1:200).

in 15 min, 1 mL/min); retention time = 4.8 min. **HPMAm-Bz**: (5−95% solvent B in 15 min, 1 mL/min); retention time = 9.8 min.

For PTX, an Acquity UPLC BEH C18 column (2.1 mm × 50 mm, 1.7 μm) as the stationary phase and isocratic elution of ACN/H_2O (40/60% v/v, containing 0.1% TFA) as the mobile phase were employed. The injection volume was 2 μL with a 0.8 mL/min flow rate. The detector wavelength was 227 nm. The retention time was 2.3 min.

Micelle Preparation. Empty and PTX-loaded polymeric micelles were prepared via a nanoprecipitation method.[17] To this end, 10 mg of mPEG-*b*-p(HPMAm-Bz) block copolymers (and 1 mg of PTX in the case of drug-loaded) were dissolved in 1 mL of THF. The solutions were dropwise added to 1 mL of Milli-Q water under stirring at 1000 rpm. The samples were kept at room temperature for 24 h to allow for THF evaporation. The volume of the micellar dispersions was adjusted to 1 mL with Milli-Q water and micellar dispersions were filtered through a 0.45 μm polyethersulfone (PES) disk filter before analysis. For drug-loaded micelles, the encapsulation efficiency (EE) and loading capacity (LC) were calculated using eqs 2 and 3, respectively:

$$\mathrm{EE}(\%) = \frac{\text{concentration of the loaded PTX into the micelles}}{\text{feed concentration of PTX}} \times 100\% \quad (2)$$

$$\mathrm{LC}(\%) = \frac{\text{concentration of the loaded PTX into the micelles}}{\text{concentration of the loaded PTX and polymer}} \times 100\% \quad (3)$$

Dynamic Light Scattering (DLS). The hydrodynamic diameter (size) and polydispersity index (PDI) of the micelles were measured by DLS (Nano-S, Malvern Panalytical PLC), using disposable polystyrene cuvettes. The samples were diluted to 500 μg/mL of polymer using Milli-Q water before measurement. Samples were measured at a fixed scattering angle of 173° and a temperature of 25 °C. The attenuator was automatically chosen for measurements.

Transmission Electron Microscopy (TEM). For TEM analysis, micellar dispersions (10 mg/mL) were diluted 100 times with water. The samples were left to adsorb on glow discharged Formvar-carbon-coated nickel grids (Maxtaform, 200 mesh) for 10 min. Negative staining was performed with 0.5% uranyl acetate (Science Services GmbH). TEM images were recorded on a TEM LEO 906 (Carl Zeiss), operating at an acceleration voltage of 60 kV.

Critical Micelle Concentration (CMC). The CMC of the polymers was determined using pyrene as a fluorescent probe.[22] In brief, serial dilutions of micelles were prepared in water. Next, 6 μL of pyrene in acetone (1.8×10^{-4} M) was added to 1.5 mL of the micellar dispersions. The dispersions were subsequently incubated for 20 h at room temperature in the dark and fluorescence excitation spectra of pyrene were recorded via a spectrofluorometer (Tecan infinite m200 pro) at a 90° angle. The excitation spectra (300 to 360 nm with emission wavelength of 390 nm) were recorded while excitation and emission band slits were 4 and 2 nm, respectively. The ratio of excitation intensity at 338 nm to that at 333 nm was plotted against the concentration of the polymer to determine the CMC.

Nanoparticle Tracking Analysis (NTA). The concentration of particles in the micellar dispersions was measured via NTA using a NanoSight instrument (Malvern Panalytical PLC). Micellar dispersions (concentration 10 mg/mL) were diluted 500 times in Milli-Q water. Nanoparticles were visualized via scattered light from a blue laser (488 nm) and a 60 s video for each sample was recorded via sCMOS camera. NTA 3.2 software was used for the analysis of the data.

Stability Study. The stability of empty polymeric micelles was monitored using DLS by incubating them in phosphate buffered saline (PBS, composition: 137.9 mM sodium chloride, 1.47 mM potassium phosphate monobasic, 2.67 mM potassium chloride, 8.09 mM sodium phosphate dibasic) at pH 7.4 and 37 °C for 2 weeks. Samples were taken at different time points and analyzed for size and PDI.

Drug Release. Drug release of PTX-loaded micelles was evaluated under sink conditions in PBS (pH 7.4) containing 45 mg/mL bovine serum albumin (BSA).[23] In brief, Float-A-Lyzer dialysis devices (MWCO of 300 kDa) were filled with 1 mL of PTX-loaded micelles and submerged in the medium at 37 °C under shaking agitation. At

https://doi.org/10.1021/acs.biomac.2c01261
Biomacromolecules 2023, 24, 4444−4453

different time points, samples of 50 μL were withdrawn from the dialysis device, diluted 10 times in ACN, centrifuged at 5000 g for 10 min to remove the precipitated BSA, and the PTX content in the supernatant was determined via HPLC. The withdrawn volumes were compensated with equal volumes of BSA in PBS solution.

Cytotoxicity. Cytotoxicity of the large FR and RAFT polymers was evaluated in LL-PK1 (ATCC CL-101, porcine epithelial kidney cell) and Hep G2 (ATCC HB-8065, human hepatocyte carcinoma cell) cell lines. LLC-PK1 cells were cultivated in Medium 199 supplemented with 3% v/v fetal bovine serum (FBS), 2 mM L-glutamine, and 100 units/mL penicillin/streptomycin. Hep G2 cells were cultured in RPMI 1640 supplemented with 10% v/v FBS, 2 mM L-glutamine, and 100 units/mL penicillin/streptomycin. Both cell lines were cultivated in 96-well plates in humidified atmosphere at 37 °C and 5% CO_2 overnight. Afterward, the FR and RAFT polymers (dissolved in media containing ≤1% DMSO, with concentrations below and above CMC) were incubated with the cells for 24 h. Cell culture medium was exchanged, MTT reagent (3-(4,5-dimethyl-2-thiazolyl)-2,5-diphenyl-2*H*-tetrazolium bromide) was added and the cells were incubated for 4 h at 37 °C. The medium was replaced by 200 μL DMSO and 25 μL of glycine buffer (pH 10.5, 0.1 M) and the absorbance at 570 nm was measured using a plate reader.

RESULTS AND DISCUSSION

Optimization of RAFT Polymerization Conditions for HPMAm-Bz. In order to find suitable conditions for RAFT polymerization of HPMAm-Bz, we first evaluated the effect of different parameters (solvent, monomer concentration, molar ratio of CTA to initiator, and molar ratio of CTA to monomer) on the monomer conversion and dispersity of the p(HPMAm-Bz) homopolymers. DMSO and dioxane were selected as two solvents that dissolve all the reagents. A constant monomer:CTA:AIBN molar ratio of 100:1:0.2 was used and two monomer concentrations (1 and 2 M) were tested. In all the experiments, the monomer conversions were between 60% and 85% after 24 h of reaction, while all the polymers demonstrated low dispersities ($Đ \leq 1.5$) (Figure 1A). Reaction conditions of 2 M monomer concentration in DMSO were chosen for the rest of the experiments as it resulted in the highest monomer conversion, and as DMSO is considered a safer solvent compared to dioxane (class 3 versus class 2 solvent). Subsequently, three different molar ratios of CTA to initiator (i.e., 1:0.2, 1:0.1, and 1:0.05) were investigated using 2 M monomer concentration in DMSO. The molar ratio of 1:0.05 resulted in the lowest monomer conversion (around 30%) after 48 h of reaction, while the ratios of 1:0.2 and 1:0.1 led to considerably higher monomer conversions (around 85% and 75%, respectively) (Figure 1B). Finally, the effect of the molar ratio of CTA to monomer (i.e., 1:200, 1:100, and 1:50) on polymerization kinetics and conversion was studied using 2 M monomer concentration and CTA:initiator ratio of 1:0.2 in DMSO. A ratio of 1:200 resulted in a low monomer conversion of around 20% after 24 h of reaction, while ratios of 1:100 and 1:50 resulted in conversion rates of above 80% during the same reaction time (Figure 1C).

Reactions in all the evaluated conditions resulted in polymers with low dispersities ($Đ \leq 1.5$). To narrow down the selection to one condition for the rest of the study, kinetic constants (k) of different reaction conditions were calculated and compared against each other (Table 1). The kinetic constants were calculated from the linear fitting of ln([Mo]/[Mt]) over time (Figure S1). Among different conditions evaluated, reactions in DMSO as a solvent, with 2 M monomer concentration, CTA to initiator (AIBN) molar ratio of 1:0.2 and CTA to monomer molar ratios of 1:50 and 1:100 led to the highest monomer conversion and fastest polymerizations (k of 0.095 and 0.084 h^{-1}, respectively). As the CTA to monomer molar ratio of 1:50 resulted in a lower degree of polymerization, CTA to monomer molar ratio of 1:100 was identified as the most suitable for RAFT polymerization of HPMAm-Bz.

Table 1. First-Order Kinetic Constants (k) of RAFT Polymerization of HPMAm-Bz under Different Conditions[a]

Solvent	Monomer concentration (M)	CTA:Initiator (mol/mol)	CTA:Monomer (mol/mol)	k (h^{-1})
Dioxane	1	1:0.2	1:100	0.051
	2	1:0.2	1:100	0.072
DMSO	1	1:0.2	1:100	0.066
	2	1:0.2	1:100	0.084
	2	1:0.2	1:200	0.011
	2	1:0.2	1:50	0.095
	2	1:0.05	1:100	0.017
	2	1:0.1	1:100	0.061

[a]Kinetic constants were calculated based on a first-order kinetic model, following eq 1 in the Experimental Section.

Comparison of mPEG-*b*-p(HPMAm-Bz) Block Copolymers Synthesized via FR and RAFT Polymerization. mPEG-*b*-p(HPMAm-Bz) block copolymers were then synthesized via FR polymerization following a previously established protocol[17] (Scheme 1A) and via RAFT polymerization using the chosen conditions: 2 M monomer concentration with monomer:CTA:initiator ratio of 100:1:0.2 in DMSO (Scheme 1B). The FR polymerization reaction resulted in a ^{1}H NMR-based monomer conversion of roughly 80% after 12 h of reaction, with a kinetic constant (k) of 0.116 h^{-1} (Figure 2A and C). RAFT polymerization led to similar kinetics (k of 0.096 h^{-1}) and a comparable monomer conversion of around 70% after the same reaction time (Figure 2B and D).

The obtained polymers were characterized by GPC (Figure 2E and F, darker shades indicate polymers with longer reaction times). In FR polymerization, a new peak (retention time around 12.5 min) appeared in the chromatogram next to the macroinitiator peak (retention time around 14 min). Over the course of the reaction, the new peak did not shift (no change in MW), and only the ratio of the area of the new peak to that of the macroinitiator increased, implying that, as the reaction proceeded, more starting materials (monomer and macroinitiator) were consumed to produce higher amounts of mPEG-*b*-p(HPMAm-Bz) block copolymers (Figure 2E). Contrarily, GPC results of the block copolymers obtained via RAFT demonstrate that, as the reaction progressed over time, more monomers were gradually incorporated into the existing polymer chains, leading to an increase in MW of the product mixture (Figure 2F). Overall, the results confirm that RAFT polymerization can be successfully employed for the synthesis of mPEG-*b*-p(HPMAm-Bz) with a good control over polymers chain growth and thus over their MW during the reaction, which is not achievable by FR polymerization.

Synthesis of mPEG-*b*-p(HPMAm-Bz) Block Copolymers of Different Molecular Weights via FR and RAFT Polymerization. Subsequently, mPEG-*b*-p(HPMAm-Bz) block copolymers of three different chain lengths of the hydrophobic block, and thus three different overall MW, were synthesized via FR and RAFT polymerization in order to systematically evaluate the effect of the polymerization method on the characteristics of the resulting polymers. To synthesize

https://doi.org/10.1021/acs.biomac.2c01261
Biomacromolecules 2023, 24, 4444−4453

Scheme 1. Synthesis of mPEG-*b*-p(HPMAm-Bz) Block Copolymer via FR and RAFT Polymerization[a]

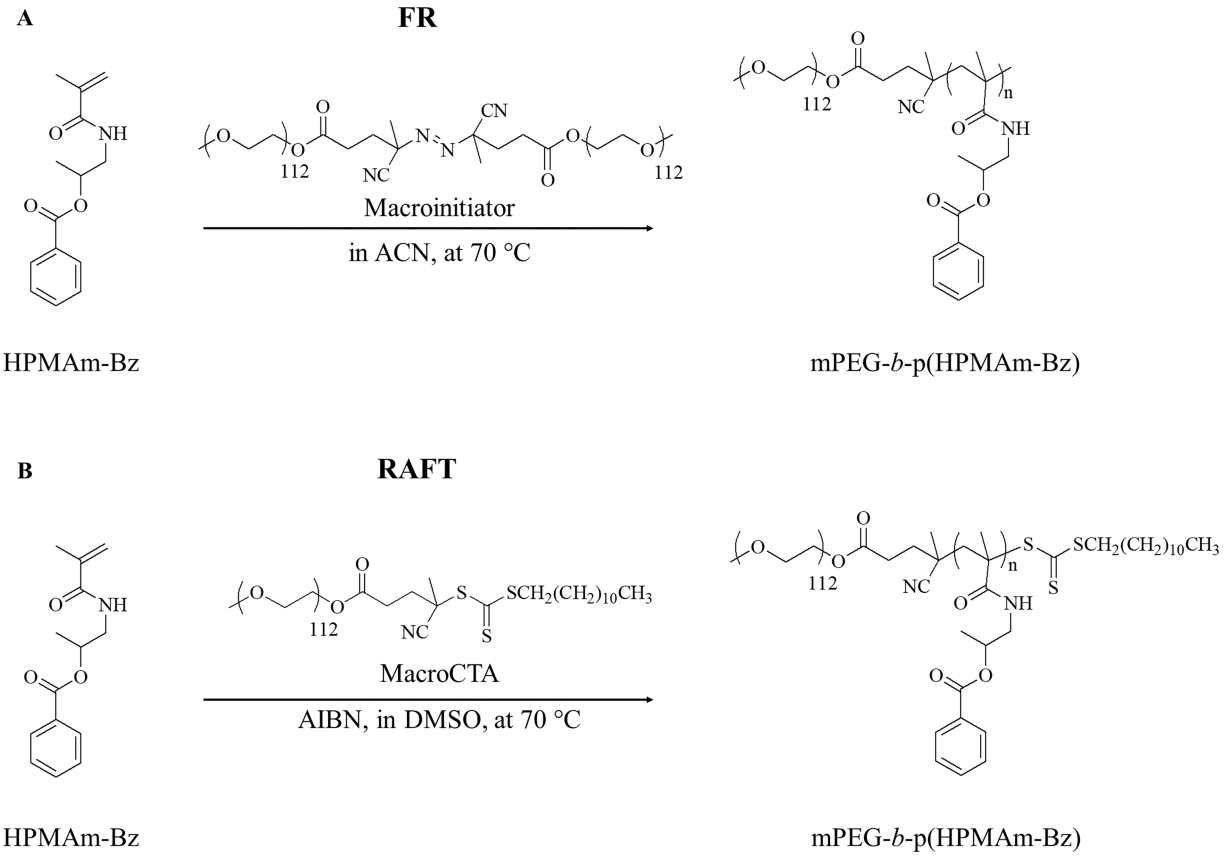

[a](A) Synthetic scheme for FR polymerization, using mPEG-ABCPA-mPEG as the macroinitiator. (B) Synthetic scheme for RAFT polymerization, using mPEG-CTA as the macroCTA.

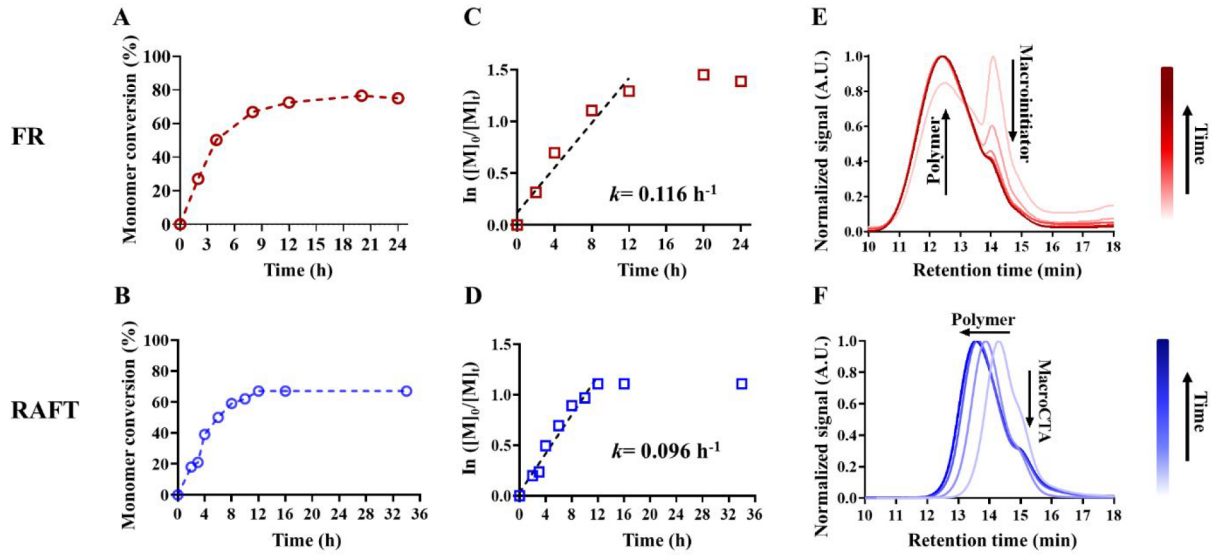

Figure 2. Reaction kinetics of mPEG-*b*-p(HPMAm-Bz) synthesis via FR and RAFT polymerization. (A–B) Monomer conversion (based on ^{1}H NMR) for FR (A) and RAFT (B) as a function of polymerization time. (C–D) Polymerization kinetics analysis, performed via monitoring the evolution of $\ln([M]_0/[M]_t)$ over reaction time for FR (C) and RAFT (D). (E–F) GPC results of the polymers obtained by FR (E) and RAFT (F) polymerization over time. Darker shades indicate polymers obtained after longer reaction times.

polymers with different MW via FR polymerization, different molar ratios of macroinitiator to monomer (1:200, 1:100, and 1:50) were used. In the case of RAFT polymerization, the block copolymers with three different MW were obtained by terminating the reaction at different times. The FR and RAFT polymer products with the three different MW (referred to as large, medium, and small) were characterized by ^{1}H NMR and GPC (Table 2 and Figures S3–S5). NMR spectra analysis

https://doi.org/10.1021/acs.biomac.2c01261
Biomacromolecules 2023, 24, 4444–4453

Table 2. Characteristics of mPEG-*b*-p(HPMAm-Bz) Block Copolymers with Different Molecular Weight Synthesized by FR and RAFT Polymerization

Polymerization route	Polymer name	Degree of polymerization ^{1}H NMR	Monomer conversion (%) ^{1}H NMR	M_n (kDa) ^{1}H NMR	M_n (kDa) GPC	Đ GPC
FR	FR-small	21	95	9	10	1.5
	FR-medium	32	69	12	11	1.7
	FR-large	67	70	22	17	1.7
RAFT	RAFT-small	21	21	9	7	1.1
	RAFT-medium	36	39	14	8	1.2
	RAFT-large	63	61	21	10	1.3

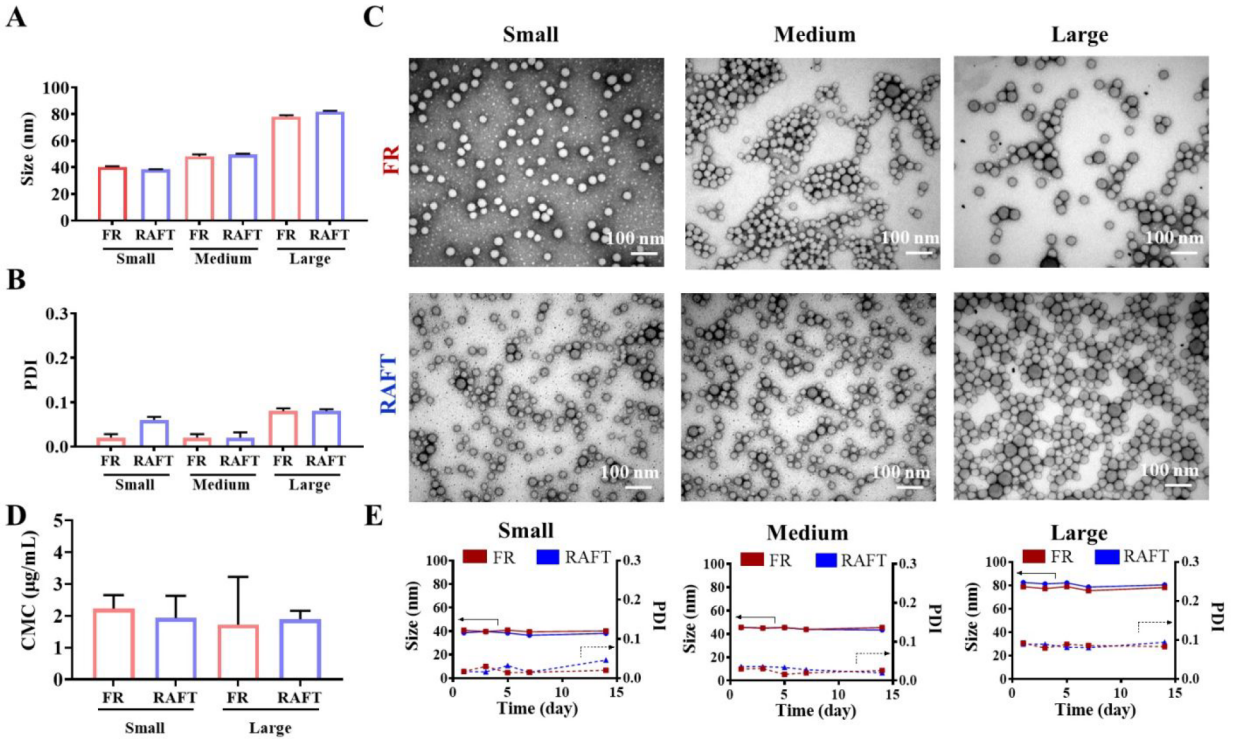

Figure 3. Pharmaceutical properties of empty polymeric micelles based on polymers of different MW synthesized by FR and RAFT polymerization. (A–B) Size (A) and PDI (B) of micelles based on small, medium and large polymers, measured by DLS. (C) TEM images of negatively stained micelles based on small, medium, and large polymers. (D) CMC values for small and large polymers. (E) Colloidal stability of micelles based on small, medium, and large polymers in PBS (pH 7.4) at 37 °C over 2 weeks. 10 mg of polymer was used to prepare 1 mL of micellar dispersion.

demonstrates that polymers synthesized exploiting the two polymerization methods had similar degree of polymerization for each MW group (around 20, 35, and 65 for small, medium, and large polymers, respectively). Importantly, the polymers synthesized via RAFT exhibited a remarkably lower dispersity than those from FR polymerization according to GPC analysis (Đ values of 1.1–1.3 versus 1.5–1.7). This is in line with expectations that polymers with narrower weight distribution can be produced by RAFT as compared to FR polymerization.[12]

The cytotoxicity of the large polymers obtained by FR and RAFT polymerization was evaluated in two different cell lines (i.e., LLC-PK1 (porcine kidney) and Hep G2 (hepatocarcinoma)). The results demonstrate that polymers obtained from the two mentioned methods have similarly high cytocompatibility within the evaluated concentration range (Figure S6).

Preparation of Micelles Based on mPEG-*b*-p(HPMAm-Bz) Block Copolymers Synthesized via FR and RAFT Polymerization. Polymers of the three different MW synthesized by FR and RAFT polymerization were used to prepare empty micelles via nanoprecipitation and the pharmaceutical properties of the micelles were assessed. Nanoprecipitation did not result in the formation of large polymer aggregates as no difference in size, size distribution, and polymer content of the micellar dispersion was observed before and after filtration of the dispersion (Figure S7). Both FR and RAFT polymers of similar MW formed micelles of similar sizes, with small, medium, and large polymers producing micelles with ∼40, ∼50, and ∼80 nm hydrodynamic diameter, respectively (Figure 3A). Thus, polymers with longer hydrophobic blocks produced micelles of larger size, which is in line with previous observations.[24,25] Interestingly and counterintuitively, even though the FR polymers had considerably higher dispersity (Đ), they formed micelles with similarly low polydispersity (PDI < 0.1), or even lower in the case of the micelles formed by the small polymers, than their RAFT counterparts (Figure 3B). This demonstrates that the size and size distribution of the polymeric micelles are not dependent on the molecular weight distribution of the polymers from which they are made. TEM images confirmed

https://doi.org/10.1021/acs.biomac.2c01261
Biomacromolecules 2023, 24, 4444–4453

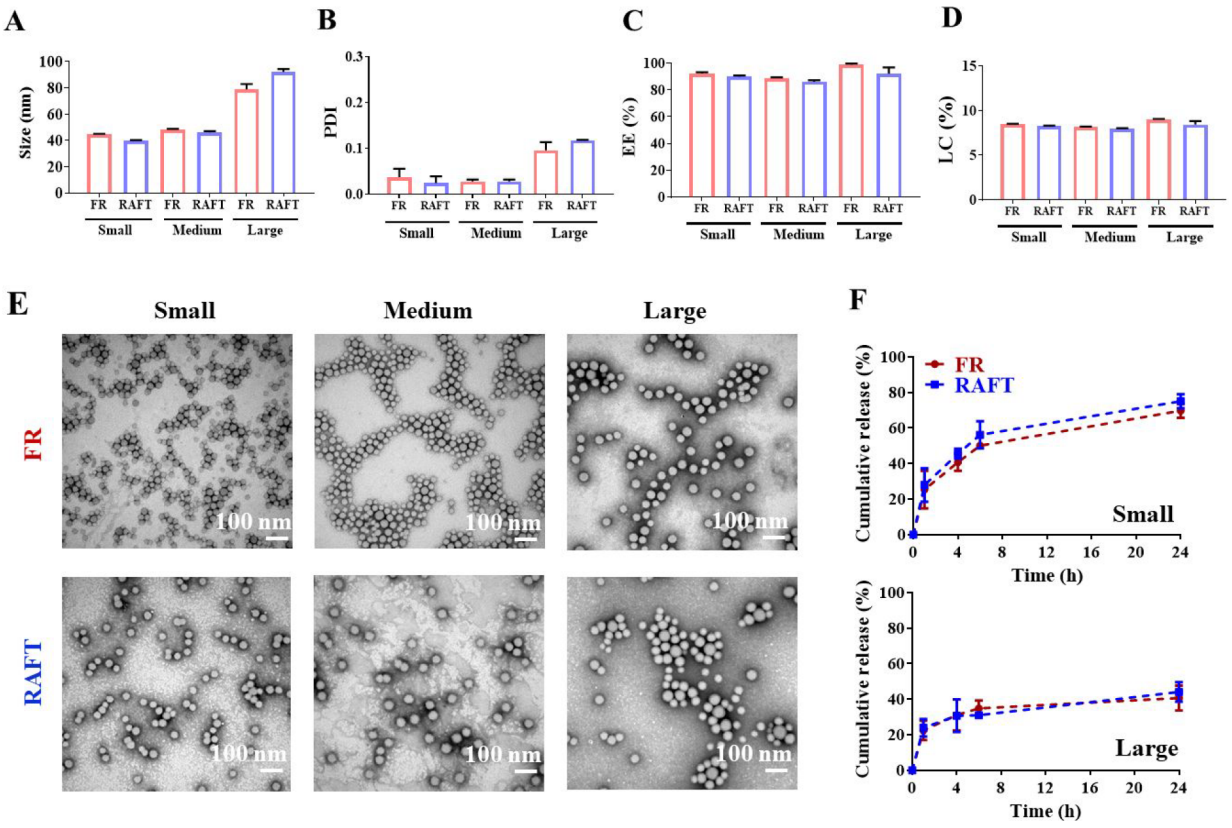

Figure 4. Paclitaxel-loaded micelles based on FR and RAFT polymers. (A–B) Size (A) and PDI (B) of the micelles measured by DLS. (C–D) PTX EE (C) and LC (D) of the micelles. (E) TEM images of negatively stained small, medium, and large micelles. (F) PTX release under sink conditions (in PBS, pH 7.4 containing 45 mg/mL of BSA) of micelles based on small and large polymers. 10 mg of polymers and 1 mg of PTX were used to prepare 1 mL of micelles.

the similar spherical morphology and homogeneity of the micelles based on both FR and RAFT polymers (Figure 3C). To investigate whether FR- and RAFT-based polymeric micelles have different stability upon dilution, the CMC of small and large polymers was measured using pyrene as fluorescent dye.[22] Micelles from both small and large polymers synthesized by FR and RAFT had similar stability with CMC values of approximately 2 μg/mL for all polymers (Figure 3D). Furthermore, stability of the micelles was evaluated in PBS (pH 7.4) at 37 °C over the course of 14 days. Micelles of the different sizes remained stable with no change in their size and PDI during this period. Thus, no obvious difference was observed between FR- and RAFT-based polymeric micelles in this regard (Figure 3E).

Comparison of Pharmaceutical Properties of Paclitaxel-Loaded Micelles Prepared Using FR and RAFT Polymers. PTX-loaded polymeric micelles were prepared using the polymers synthesized via FR and RAFT polymerization, and their pharmaceutical properties were analyzed and compared. Polymers with three different MW were used to prepare PTX-loaded micelles of small, medium, and large size. The encapsulation efficiencies (EE) of PTX reached around 90% and the loading capacity (LC) was approximately 8% for all of the micelles (Figure 4C and D), suggesting that PTX can be efficiently loaded into the micelles regardless of the hydrophobic block size of the polymer or its method of preparation. DLS analysis showed that these micelles (small, medium, and large) had a size of around 45, 50, and 80 nm, respectively (Figure 4A). The drug-loaded micelles had similar sizes to the empty ones, likely because of the low feed amount of PTX. Figure 4B shows that all of the PTX-loaded micelles, regardless of their forming polymers, had low PDI (around or below 0.1), and that there was no obvious difference between the micelles of different polymerization origin. Overall, the DLS results point out to equivalent characteristics between micelles prepared from FR and RAFT polymers of analogous MW.

Given that the concentration of particles can eventually impact the biodistribution and target-site accumulation of drug delivery systems,[26] nanoparticle tracking analysis (NTA) was used to determine and compare the concentration of particles in FR- and RAFT-based micelles of large size (Figure S8). NTA analysis demonstrated concentrations of $(6.7 \pm 0.1) \times 10^{11}$ and $(4.9 \pm 0.1) \times 10^{11}$ particles/mL for micelles based on large FR and RAFT polymers, respectively. Given that both values are within the same order of magnitude, the concentration of the self-assemblies in both FR and RAFT polymers can be considered similar. Furthermore, as observed from the TEM images, the polymerization method used for the synthesis of the block copolymers did not have an impact on the spherical morphology of the drug-loaded micelles either (Figure 4E).

Lastly, PTX release profile was evaluated for small and large micelles in 45 mg/mL BSA solution in PBS under sink conditions (Figure 4F). Release studies under similar conditions have recently been shown to adequately predict in vivo blood circulation of the drugs loaded in such polymeric micelles.[27] PTX release from large micelles was slower than

https://doi.org/10.1021/acs.biomac.2c01261
Biomacromolecules 2023, 24, 4444–4453

that of the small ones, with around 45% and 75% of PTX released within 24 h, respectively. This finding is in line with previous results showing that the PTX retention capability of mPEG-*b*-p(HPMAm-Bz)-based micelles is dependent on the size of the hydrophobic block of the copolymer.[23] Furthermore, there was no difference in terms of PTX release profile between micelles prepared from FR and RAFT polymers, implying that micelles prepared from polymers of the two methods would potentially have similar PTX retention profile in the bloodstream.

Collectively, we found that, in spite of the obvious difference in the dispersity of mPEG-*b*-p(HPMAm-Bz) synthesized by FR and RAFT polymerization, they formed micelles of similar size and size distribution. Furthermore, drug loading and retention properties of PTX-containing micelles based on FR and RAFT polymers of similar MW were not different from each other. Although it was hypothesized that controlled/living polymerization techniques such as RAFT and atom transfer radical polymerization (ATRP) yield polymers with a narrow molecular weight distribution that in turn result in polymeric micelles with a low PDI, our findings do not support this. In the recent report of Buckinx and colleagues, the effect of polymer dispersity on the size and size distribution of their self-assemblies was evaluated.[15] They synthesized block copolymers comprised of hydroxy ethyl acrylate as the hydrophilic block and polystyrene (with different dispersities) as the hydrophobic block. Interestingly, increasing the dispersity of the core-forming hydrophobic block led to self-assemblies with lower polydispersity. Moreover, the authors showed that the size of self-assemblies decreased as the dispersity of the hydrophobic block increased, pointing toward more efficient and compact core formation in less homogeneous copolymers. While their work also demonstrates that more homogeneous polymers do not directly translate into more monodispersed polymeric micelles, our results are not following the same trend as those reported by Buckinx et al. This discrepancy may result from the different chemical composition of the two copolymer systems. The differences in the bulkiness/sterics and chain flexibility of the two block copolymers can contribute significantly to their self-assembly behavior and the corresponding polymeric micelle properties. Overall, findings from both studies exemplify that a low dispersity of micelle-forming copolymers does not directly give rise to self-assemblies with lower polydispersity.

Our findings are highly relevant for pharmaceutical development of polymeric micelle-based drug formulations. RAFT polymerization offers the possibility of synthesizing complex polymer structures with better control over the MW and molecular weight distribution. Contrarily, FR polymerization does not provide scrupulous control from a chemical structure standpoint, while its well-established procedure, low cost, and ease of scalability are still appealing traits for the design, industrial development, and eventually clinical translation of polymer-based nanoparticles.[28] Compared to the conventional FR polymerization, RAFT polymerization requires the addition of another component (CTA) in the reaction mixture, which can entail some disadvantages in certain applications or further processing. Thus, it might require modification or removal from the final product. Such extra steps may impose additional burdens in terms of cost and convenience for upscaling in comparison to the conventional FR polymerization.[29] Having demonstrated similar pharmaceutical properties from micelles of FR and RAFT polymer origin, our results can assist future upscaling of polymer synthesis and the corresponding micelle formulation; implying that other factors besides low dispersity of the produced polymers such as cost-effectiveness and ease of scalability should also be taken into account when choosing the polymerization method for preparing polymeric micelles.

CONCLUSION

Our study shows that even though mPEG-*b*-p(HPMAm-Bz) copolymers synthesized via RAFT polymerization have lower dispersities compared to their FR counterparts, micelles prepared from polymers of both methods display similar size, size distribution, cytocompatibility, and drug loading and retention capabilities. As opposed to the existing desire for synthesizing polymers with a narrow molecular weight distribution, low dispersity may not necessarily translate into micellar self-assemblies with better pharmaceutical properties. Thus, other factors such as cost-effectiveness and ease of scalability are also important to be considered when choosing the polymerization method for preparing polymeric micelles.

ASSOCIATED CONTENT

Supporting Information

The Supporting Information is available free of charge at https://pubs.acs.org/doi/10.1021/acs.biomac.2c01261.

Polymerization kinetics of homopolymer, GPC chromatogram of macroCTA and polymers, NMR spectra of the polymers, cell viability, DLS and GPC spectra of micelles without and with filtration, and NTA images (PDF)

AUTHOR INFORMATION

Corresponding Authors

Twan Lammers − *Institute for Experimental Molecular Imaging, RWTH Aachen University Hospital, 52074 Aachen, Germany;* orcid.org/0000-0002-1090-6805; Email: tlammers@ukaachen.de

Quim Peña − *Institute for Experimental Molecular Imaging, RWTH Aachen University Hospital, 52074 Aachen, Germany;* orcid.org/0000-0001-6477-8127; Email: jpena@ukaachen.de

Yang Shi − *Institute for Experimental Molecular Imaging, RWTH Aachen University Hospital, 52074 Aachen, Germany;* orcid.org/0000-0003-4530-2056; Email: yshi@ukaachen.de

Authors

Armin Azadkhah Shalmani − *Institute for Experimental Molecular Imaging, RWTH Aachen University Hospital, 52074 Aachen, Germany;* orcid.org/0000-0003-2238-6525

Zaheer Ahmed − *Institute for Experimental Molecular Imaging, RWTH Aachen University Hospital, 52074 Aachen, Germany*

Maryam Sheybanifard − *Institute for Experimental Molecular Imaging, RWTH Aachen University Hospital, 52074 Aachen, Germany*

Alec Wang − *Institute for Experimental Molecular Imaging, RWTH Aachen University Hospital, 52074 Aachen, Germany;* orcid.org/0000-0001-5198-559X

Marek Weiler − *Institute for Experimental Molecular Imaging, RWTH Aachen University Hospital, 52074 Aachen, Germany*

https://doi.org/10.1021/acs.biomac.2c01261
Biomacromolecules 2023, 24, 4444−4453

Eva Miriam Buhl − *Electron Microscopy Facility, Institute of Pathology, RWTH University Hospital, 52074 Aachen, Germany*
Geir Klinkenberg − *Department of Biotechnology and Nanomedicine, SINTEF Industry, 7034 Trondheim, Norway*
Ruth Schmid − *Department of Biotechnology and Nanomedicine, SINTEF Industry, 7034 Trondheim, Norway*
Wim Hennink − *Department of Pharmaceutics, Utrecht Institute for Pharmaceutical Sciences, Faculty of Science, Utrecht University, 3508 TB Utrecht, The Netherlands;* orcid.org/0000-0002-5750-714X
Fabian Kiessling − *Institute for Experimental Molecular Imaging, RWTH Aachen University Hospital, 52074 Aachen, Germany;* orcid.org/0000-0002-7341-0399
Josbert M. Metselaar − *Institute for Experimental Molecular Imaging, RWTH Aachen University Hospital, 52074 Aachen, Germany*

Complete contact information is available at: https://pubs.acs.org/10.1021/acs.biomac.2c01261

Author Contributions

#The manuscript was written through contributions of all authors. All authors have given approval to the final version of the manuscript. AAS and ZA contributed equally to this paper.

Notes

The authors declare no competing financial interest.

■ ACKNOWLEDGMENTS

The authors are grateful for financial support by the German Research Foundation (DFG: SH1223/1-1; LA2937/4-1; GRK/RTG 2735 (project number 331065168)), the German Federal Ministry of Research and Education (BMBF: Gezielter Wirkstofftransport, PP-TNBC, Project No. 16GW0319K), Higher Education Commission of Pakistan and German Academic Exchange Services (HEC-DAAD Pakistan), and the European Research Council (ERC: Meta-Targeting (864121); BeaT-IT (101040996)).

■ REFERENCES

(1) Mitchell, M. J.; Billingsley, M. M.; Haley, R. M.; Wechsler, M. E.; Peppas, N. A.; Langer, R. Engineering Precision Nanoparticles for Drug Delivery. *Nat. Rev. Drug Discovery* **2021**, *20*, 101−124.
(2) Mast, M. P.; Modh, H.; Champanhac, C.; Wang, J. W.; Storm, G.; Krämer, J.; Mailänder, V.; Pastorin, G.; Wacker, M. G. Nanomedicine at the Crossroads − A Quick Guide for IVIVC. *Adv. Drug Delivery Rev.* **2021**, *179*, 113829.
(3) Gadekar, V.; Borade, Y.; Kannaujia, S.; Rajpoot, K.; Anup, N.; Tambe, V.; Kalia, K.; Tekade, R. K. Nanomedicines Accessible in the Market for Clinical Interventions. *J. Controlled Release* **2021**, *330*, 372−397.
(4) Younis, M. A.; Tawfeek, H. M.; Abdellatif, A. A. H.; Abdel-Aleem, J. A.; Harashima, H. Clinical Translation of Nanomedicines: Challenges, Opportunities, and Keys. *Adv. Drug Delivery Rev.* **2022**, *181*, 114083.
(5) Ghezzi, M.; Pescina, S.; Padula, C.; Santi, P.; del Favero, E.; Cantù, L.; Nicoli, S. Polymeric Micelles in Drug Delivery: An Insight of the Techniques for Their Characterization and Assessment in Biorelevant Conditions. *J. Controlled Release* **2021**, *332*, 312−336.
(6) Cabral, H.; Miyata, K.; Osada, K.; Kataoka, K. Block Copolymer Micelles in Nanomedicine Applications. *Chem. Rev.* **2018**, *118*, 6844−6892.
(7) Hwang, D.; Ramsey, J. D.; Kabanov, A. v. Polymeric Micelles for the Delivery of Poorly Soluble Drugs: From Nanoformulation to Clinical Approval. *Adv. Drug Delivery Rev.* **2020**, *156*, 80−118.
(8) Varela-Moreira, A.; Shi, Y.; Fens, M. H. A. M.; Lammers, T.; Hennink, W. E.; Schiffelers, R. M. Clinical Application of Polymeric Micelles for the Treatment of Cancer. *Mater. Chem. Front* **2017**, *1*, 1485−1501.
(9) Houdaihed, L.; Evans, J. C.; Allen, C. Overcoming the Road Blocks: Advancement of Block Copolymer Micelles for Cancer Therapy in the Clinic. *Mol. Pharmaceutics* **2017**, *14*, 2503−2517.
(10) Ghezzi, M.; Pescina, S.; Padula, C.; Santi, P.; del Favero, E.; Cantù, L.; Nicoli, S. Polymeric Micelles in Drug Delivery: An Insight of the Techniques for Their Characterization and Assessment in Biorelevant Conditions. *J. Controlled Release* **2021**, *332*, 312−336.
(11) Odian, G. *Principles of Polymerization*; John Wiley & Sons, Inc., 2004. DOI: 10.1002/047147875X.
(12) Truong, N. P.; Jones, G. R.; Bradford, K. G. E.; Konkolewicz, D.; Anastasaki, A. A Comparison of RAFT and ATRP Methods for Controlled Radical Polymerization. *Nat. Rev. Chem.* **2021**, *5*, 859−869.
(13) Perrier, S. 50th Anniversary Perspective: RAFT Polymerization - A User Guide. *Macromolecules* **2017**, *50*, 7433−7447.
(14) Zhao, Z.; Ukidve, A.; Krishnan, V.; Mitragotri, S. Effect of Physicochemical and Surface Properties on in Vivo Fate of Drug Nanocarriers. *Adv. Drug Delivery Rev.* **2019**, *143*, 3−21.
(15) Buckinx, A.-L.; Rubens, M.; Cameron, N. R.; Bakkali-Hassani, C.; Sokolova, A.; Junkers, T. The Effects of Molecular Weight Dispersity on Block Copolymer Self-Assembly. *Polym. Chem.* **2022**, *13*, 3444−3450.
(16) Liang, C.; Bai, X.; Qi, C.; Sun, Q.; Han, X.; Lan, T.; Zhang, H.; Zheng, X.; Liang, R.; Jiao, J.; Zheng, Z.; Fang, J.; Lei, P.; Wang, Y.; Möckel, D.; Metselaar, J. M.; Storm, G.; Hennink, W. E.; Kiessling, F.; Wei, H.; Lammers, T.; Shi, Y.; Wei, B. Π Electron-Stabilized Polymeric Micelles Potentiate Docetaxel Therapy in Advanced-Stage Gastrointestinal Cancer. *Biomaterials* **2021**, *266*, 120432.
(17) Shi, Y.; van der Meel, R.; Theek, B.; Oude Blenke, E.; Pieters, E. H. E.; Fens, M. H. A. M.; Ehling, J.; Schiffelers, R. M.; Storm, G.; van Nostrum, C. F.; Lammers, T.; Hennink, W. E. Complete Regression of Xenograft Tumors upon Targeted Delivery of Paclitaxel via Π - Π Stacking Stabilized Polymeric Micelles. *ACS Nano* **2015**, *9*, 3740−3752.
(18) Bresseleers, J.; Bagheri, M.; Storm, G.; Metselaar, J. M.; Hennink, W. E.; Meeuwissen, S. A.; van Hest, J. C. M. Scale-Up of the Manufacturing Process to Produce Docetaxel-Loaded mPEG-*b*-p(HPMA-Bz) Block Copolymer Micelles for Pharmaceutical Applications. *Org. Process Res. Dev* **2019**, *23*, 2707−2715.
(19) Palao-Suay, R.; Aguilar, M. R.; Parra-Ruiz, F. J.; Maji, S.; Hoogenboom, R.; Rohner, N. A.; Thomas, S. N.; San Román, J. α-Tocopheryl Succinate-Based Amphiphilic Block Copolymers Obtained by RAFT and Their Nanoparticles for the Treatment of Cancer. *Polym. Chem.* **2016**, *7*, 838−850.
(20) Shi, Y.; van Steenbergen, M. J.; Teunissen, E. A.; Novo, L.; Gradmann, S.; Baldus, M.; van Nostrum, C. F.; Hennink, W. E. Π-Π Stacking Increases the Stability and Loading Capacity of Thermosensitive Polymeric Micelles for Chemotherapeutic Drugs. *Biomacromolecules* **2013**, *14*, 1826−1837.
(21) Shi, Y.; van den Dungen, E. T. A.; Klumperman, B.; van Nostrum, C. F.; Hennink, W. E. Reversible Addition−Fragmentation Chain Transfer Synthesis of a Micelle-Forming, Structure Reversible Thermosensitive Diblock Copolymer Based on the N-(2-Hydroxy Propyl) Methacrylamide Backbone. *ACS Macro Lett.* **2013**, *2*, 403−408.
(22) Sun, F.; Jaspers, T. C. C.; van Hasselt, P. M.; Hennink, W. E.; van Nostrum, C. F. A Mixed Micelle Formulation for Oral Delivery of Vitamin K. *Pharm. Res.* **2016**, *33*, 2168−2179.
(23) Sheybanifard, M.; Beztsinna, N.; Bagheri, M.; Buhl, E. M.; Bresseleers, J.; Varela-Moreira, A.; Shi, Y.; van Nostrum, C. F.; van der Pluijm, G.; Storm, G.; Hennink, W. E.; Lammers, T.; Metselaar, J. M. Systematic Evaluation of Design Features Enables Efficient Selection of Π Electron-Stabilized Polymeric Micelles. *Int. J. Pharm.* **2020**, *584*, 119409.

(24) Bagheri, M.; Bresseleers, J.; Varela-Moreira, A.; Sandre, O.; Meeuwissen, S. A.; Schiffelers, R. M.; Metselaar, J. M.; van Nostrum, C. F.; van Hest, J. C. M.; Hennink, W. E. Effect of Formulation and Processing Parameters on the Size of mPEG-*b*-p(HPMA-Bz) Polymeric Micelles. *Langmuir* **2018**, *34*, 15495−15506.
(25) Wang, Y.; van Steenbergen, M. J.; Beztsinna, N.; Shi, Y.; Lammers, T.; van Nostrum, C. F.; Hennink, W. E. Biotin-Decorated All-HPMA Polymeric Micelles for Paclitaxel Delivery. *J. Controlled Release* **2020**, *328*, 970−984.
(26) Ouyang, B.; Poon, W.; Zhang, Y. N.; Lin, Z. P.; Kingston, B. R.; Tavares, A. J.; Zhang, Y.; Chen, J.; Valic, M. S.; Syed, A. M.; MacMillan, P.; Couture-Senécal, J.; Zheng, G.; Chan, W. C. W. The Dose Threshold for Nanoparticle Tumour Delivery. *Nat. Mater.* **2020**, *19*, 1362−1371.
(27) Varela-Moreira, A.; van Leur, H.; Krijgsman, D.; Ecker, V.; Braun, M.; Buchner, M.; Fens, M. H. A. M.; Hennink, W. E.; Schiffelers, R. M. Utilizing in Vitro Drug Release Assays to Predict in Vivo Drug Retention in Micelles. *Int. J. Pharm.* **2022**, *618*, 121638.
(28) Destarac, M. Controlled Radical Polymerization: Industrial Stakes, Obstacles and Achievements. *Macromol. React. Eng.* **2010**, *4*, 165−179.
(29) Destarac, M. Industrial Development of Reversible-Deactivation Radical Polymerization: Is the Induction Period Over? *Polym. Chem.* **2018**, *9*, 4947−4967.

https://doi.org/10.1021/acs.biomac.2c01261
Biomacromolecules 2023, 24, 4444−4453